Ultraviolet-induced paramagnetic centers and absorption changes in singlemode Ge-doped optical fibers

Kader Médjahdi, Aziz Boukenter and Youcef Ouerdane

Laboratoire Traitement du Signal et Instrumentation,
UMR CNRS 5516, Université J. Monnet,
18 rue Benoît Lauras Bât. F, 42000 Saint-Étienne, France
kader.medjahdi@univ-st-etienne.fr

Fabrizio Messina and Marco Cannas

Dipartimento di Scienze Fisiche ed Astronomiche
dell'Università di Palermo
Via Archirafi 36, I-90123 Palermo, Italy
fmessina@fisica-unipa.it

Abstract: We investigated the laser-energy-density dependence of absorption changes and paramagnetic centers induced by a cw Ar^+ laser operating at 5.1 eV, in both unloaded and H_2-loaded singlemode Ge-doped optical fibers. The induced absorption is measured in the blue and near ultraviolet spectral range by using the 3.1 eV photoluminescence, ascribed to Ge lone pair center (GLPC), as an *in situ* probe source. We find that the Ge(1) center (GeO_4^-) is induced upon UV exposure by electron trapping on GeO_4 precursors, where the free electrons are most likely produced by ionization of GLPC. Ge(1) is responsible of optical transmission loss of the fiber in the investigated range. Hydrogen loading strongly influences the generation efficiency of the several observed paramagnetic defects, leading in particular to passivation of radiation-induced Ge(2) centers.

© 2006 Optical Society of America

References and links

1. K.O. Hill, Y. Fujii, D.C. Johnson, and B.S. Kawasaki, "Photosensitivity in optical fiber waveguides: Application to reflection filter fabrication," Appl. Phys. Lett. **32**, 647–649 (1978).
2. A. J. Ikushima, T. Fujiwara, and K. Saito, "Silica glass: A material for photonics," J. Appl. Phys. **88**, 1201–1213 (2000).
3. P.J. Lemaire, R.M. Atkins, V. Mizrahi, and W.A. Reed, "High pressure H_2 loading as a technique for achieving ultrahigh UV photosensitivity and thermal sensitivity in GeO_2 doped optical fibres," Electron. Lett. **29**, 1191–1193 (1993).
4. H. Hosono, Y. Abe, D.L. Kinser, R.A. Weeks, and K.M.H. Kawazoe, "Nature and origin of the 5-eV band in SiO_2:GeO_2 glasses," Phys. Rev. B **46**, 11445–11451 (1992).
5. J. Nishii, N. Fukumi, H. Yamanaka, K. Kawamura, H. Hosono, and H. Kawazoe, "Photochemical reactions in GeO_2-SiO_2 glasses induced by ultraviolet irradiation: Comparison between Hg lamp and excimer laser," Phys. Rev. B **52**, 1661–1665 (1995).
6. A. Sakoh, M. Takahashi, T. Yoko, J. Nishii, H. Nishiyama, and I. Miyamoto, "Photochemical process of divalent germanium responsible for photorefractive index change in GeO_2-SiO_2 glasses," Opt. Express **11**, 2679–2688 (2003).

7. M. Fujimaki, K. Yagi, Y. Ohki, H. Nishikawa, and K. Awazu, "Laser-power dependence of absorption changes in Ge-doped SiO_2 glass induced by a KrF excimer laser," Phys. Rev. B **53**, 9859–9862 (1996).

8. M. Fujimaki, T. Watanabe, T. Katoh, T. Kasahara, N. Miyazaki, Y. Ohki, and H. Nishikawa, "Structures and generation mechanisms of paramagnetic centers and absorption bands responsible for Ge-doped SiO_2 optical-fiber gratings," Phys. Rev. B **57**, 3920–3926 (1998).

9. M. Fujimaki, T. Kasahara, S. Shimoto, N. Miyazaki, S. Tokuhiro, K.S. Seol, and Y. Ohki, "Structural changes induced by KrF excimer laser photons in H_2-loaded Ge-doped SiO_2 glass," Phys. Rev. B **60**, 4682–4687 (1999).

10. J. Nishi, K. Kintaka, H. Hosono, H. Kawazoe, M. Kato, and K. Muta, "Pair generation of Ge electron centers and self-trapped hole centers in GeO_2-SiO_2 glasses by KrF excimer-laser irradiation," Phys. Rev. B **60**, 7166–7169 (1999).

11. H. Shigemura, Y. Kawamoto, J. Nishii, and M. Takahashi, "Ultraviolet-photosensitive effect of sol-gel-derived GeO_2-SiO_2 glasses," J. Appl. Phys. **85**, 3413–3418 (1999).

12. M. Takahashi, K. Ichii, Y. Tokuda, T. Uchino, T. Yoko, J. Nishii, and T. Fujiwara, "Photochemical reaction of divalent-germanium center in germanosilicate glasses under intense near-ultraviolet laser excitation: Origin of 5.7 eV band and site selective excitation of divalent-germanium center," J. Appl. Phys. **92**, 3442–3446 (2002).

13. M.Yamaguchi, K. Saito, and A. J. Ikushima, "Formation and relaxation processes of photoinduced defects in a Ge-doped SiO_2 glass," Phys. Rev. B **66**, 132106–132110 (2002).

14. B. Poumellec, M. Douay, J.C. Krupa, J. Garapon, and P. Niay, "Comparison of UV optical absorption and UV excited luminescence behaviours in Ge doped silica under H_2 loading or CW UV laser irradiation," J. Non Cryst. Solids **317**, 319–334 (2003).

15. G. Pacchioni and C. Mazzeo, "Paramagnetic centers in Ge-doped silica: A first-principles study," Phys. Rev. B. **62**, 5452–5460 (2000).

16. T. Uchino, M. Takahashi, and T. Yoko, "Structure and formation mechanism of Ge E' center from divalent defects in Ge-doped SiO_2 glass," Phys. Rev. Lett. **84**, 1475–1478 (2000).

17. M. Kristensen, "Ultraviolet-light-induced processes in germanium-doped silica," Phys. Rev. B **64**, 144201–144213 (2001).

18. T. Uchino, M. Takahashi, and T. Yoko, "Microscopic model of photoinduced and pressure-induced UV spectral changes in germanosilicate glass," Phys. Rev. B. **65**, 172202–172206 (2002).

19. T. Tamura, G. -H. Lu, M. Kohyama, and R. Yamamoto, "E' center in Ge-doped SiO_2 glass," Phys. Rev B **70**, 153201–153205 (2004).

20. M. Svalgaard, A. Harpøth, and T. Rosbirk, "Characterization of UV written waveguides with luminescence microscopy," Opt. Express **13**, 5170-5178 (2005).

21. L. Paccou, M. Lancry, and M. Douay, "Kinetics of UV-induced blue luminescence linked with the observation of the local mean index in fiber Bragg gratings," Opt. Express **13**, 7342-7349 (2005).

22. L. Skuja, "Isoelectronic series of twofold coordinated Si, Ge, and Sn atoms in glassy SiO_2: a luminescence study," J. Non-Cryst. Solids **149**, 77–95 (1992).

23. R.A. Weeks, "Paramagnetic resonance of lattice defects in irradiated quartz," J. Appl. Phys. **27**, 1376–1381 (1956).

24. S. Agnello, R. Boscaino, M. Cannas, and F.M. Gelardi, "Instantaneous diffusion effect on spin-echo decay: Experimental investigation by spectral selective excitation," Phys. Rev. B **64**, 174423–174428 (2001).

25. E.J. Friebele, D.L. Griscom, and G.H. Siegel, "Defect centers in a germanium-doped silica-core optical fiber," J. Appl. Phys. **45**, 3424–3428 (1974).

26. T.E. Tsai, D.L. Griscom, E.J.Friebele, and J.W.Fleming, "Radiation induced defect centers in high purity *GeO_2* glass," J. Appl. Phys. **62**, 2264–2268 (1987).

27. E.V. Anoikin, A.N. Guryanov, D.D. Gusovsky, E.M. Dianov, V.M. Mashinsky, S.I. Miroshnichenko, V.B. Neustruev, and V.A. Tikhomirov, "Photoinduced defects in silica glass doped with germanium and cerium," Sov. Lightwave Commun. **1**, 129–36 (1991).

28. V.B. Neustruev, "Colour centres in germanosilicate glass and optical fibres," J. Phys.: Condens. Matter **6**, 6901-6936 (1994).

29. C.P.Slichter, "Principles of Magnetic Resonance," ISBN 962-430-004-6 Springer-Verlag Hong Kong (1991).

30. S. Agnello, R. Boscaino, M. Cannas, F.M. Gelardi, F. La Mattina, S. Grandi, and A. Magistri, "Ge related centers induced by gamma irradiation in solŰgel Ge-doped silica," J. Non Cryst. Solids **322**, 134–138 (2003).

31. A.Abragam, B.Bleaney, "Electronic paramagnetic resonance of transition ions," ISBN 0198512503 Clarendon Press, Oxford (1970).

32. J. Vitko, "ESR studies of hydrogen hyperfine spectra in irradiated vitreous silica," J. Appl. Phys. **49**, 5530–5535 (1978).

33. K. Médjahdi, F. Goutaland, A. Boukenter, and Y. Ouerdane, "Ultraviolet-induced absorption during very short continuous exposure in Ge-doped optical fiber ," J. Non-Cryst. Solids **351**, 1835–1839 (2005).
34. S. Agnello, R. Boscaino, M. Cannas, A. Cannizzo, F.M. Gelardi, S. Grandi, and M. Leone, "Temperature and excitation energy dependence of decay processes of luminescence in Ge-doped silica," Phys. Rev. B. **68**, 165201 (2003).
35. F. Messina and M. Cannas, "Hydrogen-related conversions of Ge-related point defects in silica triggered by ultraviolet laser irradiation," Phys. Rev. B. **72**, 195212 (2005).
36. K. Médjahdi, A. Boukenter and Y. Ouerdane,"Collisional deactivation mechanism of luminescence in hydrogen-loaded Ge-doped fibers," J. Chem. Phys. **123**, 214701-214704 (2005).
37. K. Awazu, H. Onuki, and K. Muta, "Mechanisms of photo-bleaching of 5 eV optical absorption band in hydrogen loaded Ge-doped SiO_2," J. Non-Cryst. Solids **211**, 158–163 (1997).
38. F. Messina and M. Cannas, "In situ observation of the generation and annealing kinetics of E' centres induced in amorphous SiO_2 by 4.7eV laser irradiation," J.Phys.: Condens. Matter **17**, 3837–3842 (2005).

1. Introduction

The effects of ultraviolet (UV) exposure on germanosilicate glasses are nowadays an open research issue strongly motivated by the many applications of these materials in photonics, ranging from standard optical fibers for telecommunications to Bragg gratings [1], nonlinear optical devices [2], *etc.*. In particular, in the last decade many studies have focused on transparency loss and photosensitivity induced by UV exposure. Considerable effort has been devoted to enhance photosensitivity in view to satisfy the practical requirements, and it has been reported that a simple but highly effective technique for achieving high UV photosensitivity is low temperature hydrogen loading prior to UV exposure [3].

Several works, both experimental [4–14] and computational [15–19], have pointed out that the UV induced change of the refractive index is related to the induced optical absorption (OA) through the Kramers-Kronig relations, and that these effects are due to generation and transformation of point defects embedded in glass matrix. Hence, the identification of defects responsible of these processes in Ge-doped glasses is a clue to make clear the microscopic origin of transparency loss and photosensitivity, in particular for the first stages of these processes occurring under very low-dose cw UV exposure ($\sim J/cm^2$).

Till now, most investigations have been performed on fiber preforms [14] or bulk glasses [4–8, 10] by the combined use of OA and electron spin resonance (ESR) techniques. The latter has provided for the structural identification of several Ge-related paramagnetic centers which contribute to the absorption over a wide region extending from visible to vacuum UV [4–13]. At variance, OA measurements on singlemode optical fibers remain difficult to perform owing to technological and physical limitations. Since these kind of fiber is used in many fields it seems important to directly examine their radiation response instead of extrapolating it from bulk and preform samples. To overcome these difficulties, we used a *moving-fiber* technique, where the 3.1 eV photoluminescence (PL) [20, 21], ascribed to GLPC [22], excited by UV laser light during exposure, is exploited as an *in situ* probe source to measure OA spectrum.

In the present study, we investigated OA and paramagnetic centers induced by laser exposure at different energy densities in both unloaded and H_2-loaded singlemode Ge-doped optical fibers. Our purpose is to get a deeper clarification of the microscopic origin of the photoinduced structural changes observed in these materials.

2. Experimental procedures

The measurements reported here were carried out at room temperature in singlemode Ge-doped optical fibers with core diameter of 4 μm. The Ge content in the fiber core is 4 mol% and the cladding is pure silica. Hydrogen loading was carried out in a vessel under a H_2 pressure of 140 atm for three weeks at room temperature, leading to a saturated concentration of 1.7 mol%.

The polymer coating was removed before transverse UV irradiation by 5.1 eV photons from a cw frequency-doubled Ar^+ laser, focused on an elliptic 60×800 μm^2 spot, with power density P from 17 to 160 W/cm^2. The induced OA was measured *in situ* during irradiation by an innovative technique in which the laser-excited PL band centered around 3.1 eV is exploited as an internal source of probe light (see Fig.1). During the transverse irradiation, the fiber is moved with constant velocity V (parallel to the
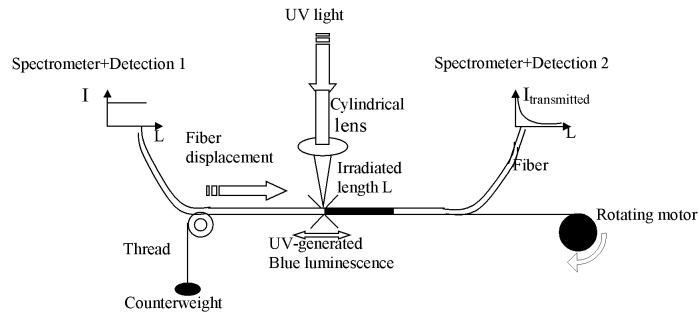

Fig. 1. Experimental set-up used to measure *in situ* the photoinduced absorption in a singlemode fiber.

shortest axes of the laser spot), between 0.2 and 1 cm/s, towards a detection system which consists of a Chromex spectrometer coupled to an Andor CCD camera (detection 2) cooled to 223 K, so that the PL propagates within the irradiated part of the fiber where it is partially absorbed. The detected amplitude reduction yields to the induced absorption coefficient over the spectral region covered by the PL band. The exposure time of a single point of the fiber to laser light is $t_e = 60$ μm/V, of the order of a few ms. To study the dependence on irradiation dose, we performed many sessions of exposure and *in situ* measurement, at different values of the laser energy density $F = P \times t_e$. This measuring method allows to combine two features: (i) irradiation of long-enough portions of fiber yields sufficient optical density permitting to obtain high-quality OA measurements and (ii) the irradiated length receives a relatively low total dose ($F \sim$J/cm^2).

ESR measurements were performed by a Bruker EMX spectrometer working at 9.7 GHz. Signal was detected on a few meters long irradiated fibers, after cutting them in portions of $\sim$0.5 cm. A microwave power $P = 1.6$ mW and a 100 kHz modulation field of peak-to-peak amplitude $B_m = 0.1$ mT were used, these values being properly chosen to avoid saturation and distortion effects in revealing the induced paramagnetic centers. Concentration of paramagnetic centers was determined by comparing the double-integrated ESR spectra with that of Si-E' centers [23], in a reference sample where their absolute density was measured with accuracy of $\pm$20% by spin-echo technique [24].

3. Results

Figure 2(a) evidences the evolution of the PL centered around 3.1 eV transmitted within
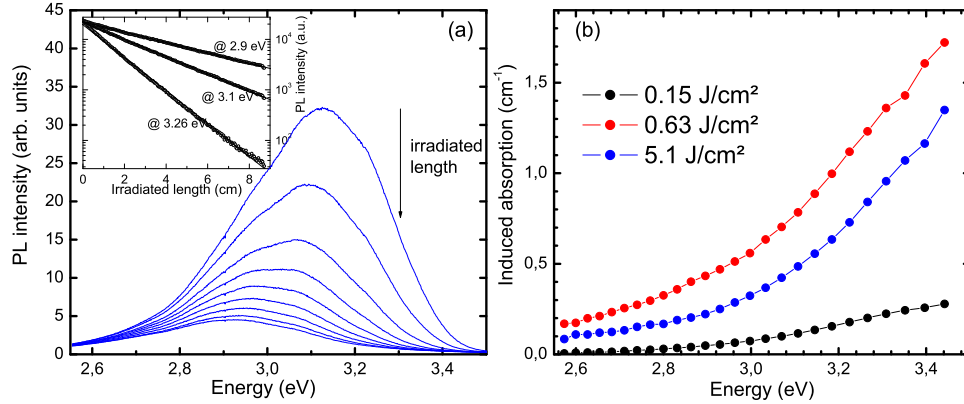

Fig. 2. (a) Evolution of laser-excited PL spectra peaked around 3.1 eV transmitted within the irradiated part of the unloaded fiber during the irradiation. The inset depicts the evolution of the PL intensity, for a given energy, as a function of the irradiated length. (b) OA spectra induced after various energy densities.

the laser-irradiated length of the unloaded optical fiber. The inset shows the decay of the PL intensity at three fixed spectral positions as a function of the fiber-irradiated length. The linear-best fitting slope gives the corresponding induced OA coefficient, which is plotted in Fig. 2(b) over the 2.56–3.44 eV range, after irradiation at three different energy densities. The induced OA increases on increasing the energy, suggesting that these curves represent the tail of an absorption band peaked at higher energy, the intensity of the band depending on energy density.

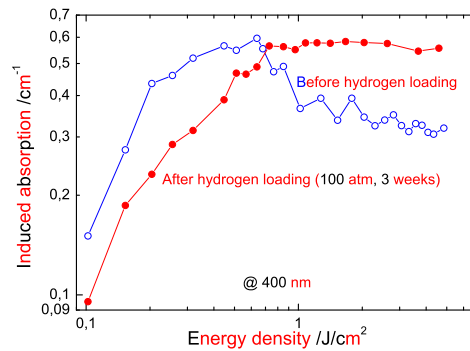Figure 3 depicts a log-log plot of the induced absorption coefficient measured at 3.1

Fig. 3. Absorption coefficient at 3.1 eV ($\Delta\alpha_{3.1}$) as a function of energy density in both unloaded and H_2-loaded fibers.

eV, $\Delta\alpha_{3.1}$, in unloaded and H_2-loaded fibers as a function of the laser-energy density ranging from 0.1 up to 5 J/cm^2. We see that the addition of hydrogen results in a reduction of the initial growth rate and in an increase of the saturation value reached at high energy densities.

ESR spectra detected in the two kinds of fibers, both exposed to a energy density of 0.8 J/cm^2, are shown in Fig. 4. It is apparent that these spectra are composite signals,
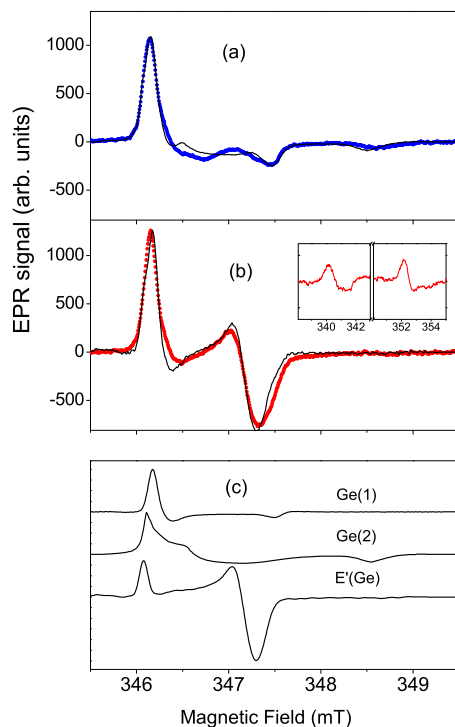

Fig. 4. ESR spectra detected in unloaded (a) and H_2-loaded (b) fibers after irradiation at 0.8 J/cm^2. Black solid lines plot the best fitting functions obtained as a linear combinations of the three base lineshapes reported in panel (c) (see text). The inset reports the ESR doublet of H(II) centers detected in H_2-loaded fibers.

resulting from the overlap of different contributions. As regards the ESR lineshapes measured in unloaded fibers [panel (a)], we found that they can be least-square-fitted, after irradiation at all energy densities, by a linear combination of the lineshapes associated with the following Ge-related paramagnetic point defects: (i) Ge(1), an electron trapped in a fourfold coordinated Ge atom, $(GeO_4)^-$ [25], (ii) GeE', an unpaired electron on a threefold coordinated Ge, $\equiv$Ge$\bullet$ [4], and iii) Ge(2). The structure of the defect responsible of the latter ESR signal is still questioned between models consisting either in a trapped electron center [10, 26] or in a hole center [8, 27, 28]. Even the circumstance that the g value of Ge(2) is smaller than 2.0023 does not permit its conclusive assignment to a trapped electron center, because this line of reasoning is rigorously valid only for very simple paramagnetic centers, and generally cannot be extended to point defects in silica [29].

The normalized ESR lineshapes of these three defects, used in the best fitting procedure, are shown separately in panel (c) of the same figure. Ge(1) and GeE' lineshapes are experimental curves measured in γ-irradiated Ge-doped samples [30], where it has been possible to single out the two defects. At variance, the Ge(2) lineshape is a curve taken from literature, obtained by Friebele *et al.* [25] by a simulation procedure aimed to fit ESR lineshapes observed in γ-irradiated multimode Ge-doped fibers.

We point out that fitting an ESR signal with a linear combination of single-defect lineshapes is founded on the assumption that the centers are sufficiently far from each other that their lineshape is not influenced by mutual interactions. This condition is usually satisfied at defects concentrations up to 10^{18}cm^{-3} [31]. Moreover, the residual discrepancies between best fit curves and experimental data are probably due both to the accuracy limit with which the three base lineshapes of panel (c) were singled out and to the presence of furhter minor contributions to the overall spectrum.

From the best fit coefficients appearing in the linear combination, we calculated the concentrations of the three defects which contribute to the overall signal measured upon exposure at each energy density.
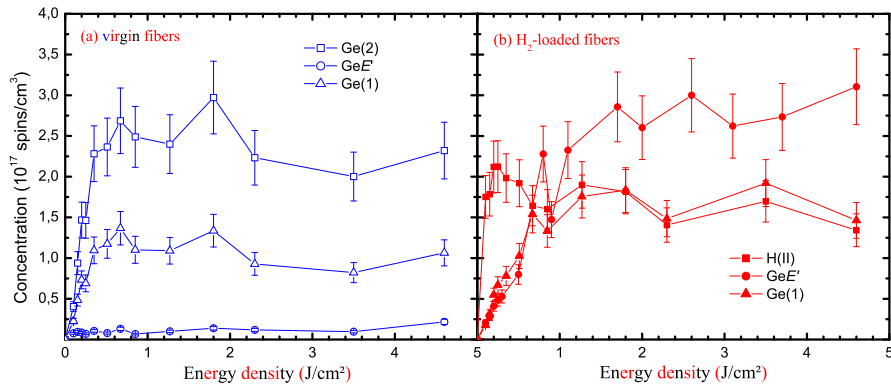

Fig. 5. Concentration of paramagnetic centers as a function of energy density detected in the two kinds of fibers.

As regards the H$_2$-loaded samples [panel (b)], the Ge(2) center is not present, as inferred from the absence of its characteristic negative peak at about 348.5 mT. So, the central portion of the spectrum mainly consists of the overlap of Ge(1) and GeE' signals whose concentration is calculated by a best fitting procedure as above described. Moreover, these samples exhibit the well-known 11.8 mT doublet [inset of panel (b)] associated with the presence of H(II) centers, =Ge$^{\bullet}$-H [32]. The concentration of H(II) has been evaluated by numerical double integration of the signal.

The obtained concentration of paramagnetic species as a function of energy density is reported in Fig. 5(a) for virgin fibers, and in Fig. 5(b) for H$_2$-loaded fibers. In the virgin fibers, the concentrations of Ge(1) and Ge(2) grow respectively to $\sim 1 \times 10^{17}$ cm^{-3} and $\sim 2 \times 10^{17}$ cm^{-3} on increasing the energy density to about 0.6 J/cm^2. The concentration [GeE'] remains much lower than the other two species. At variance, in the H$_2$-loaded samples, [GeE'] is much higher than in the virgin fiber, whereas the concentration of Ge(1) has the same order of magnitude. Finally, [H(II)] is almost constant in the investigated energy density range, suggesting its growth process to be completed at lower energy densities.

4.   Discussion

From the above reported results, we note that only Ge(1) and GeE' centers are induced in both fibers. However, while Ge(1) centers are induced in comparable amount, the concentration of GeE' is increased in presence of H_2 by a factor ~ 40. On the basis of these findings, the Ge(1) center is the only candidate to be responsible for the induced absorption in the investigated spectral range among the several observed paramagnetic centers.

To better investigate this issue, Fig. 6(a) plots the dependence between $\Delta\alpha_{3.1}$ and
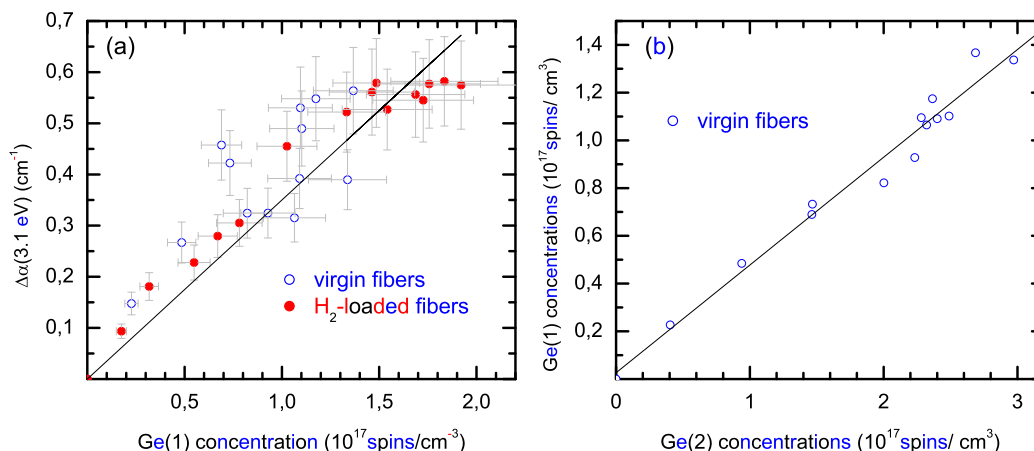

Fig. 6. (a) Correlation between concentrations of laser-induced Ge(1) centers and absorption coefficients at 3.1 eV ($\Delta\alpha_{3.1}$) measured after each sequence of irradiation. The data are taken from Figs. 3 and 5. (b) Correlation between the Ge(1) and Ge(2) centers concentrations. The open and the closed circles are for unloaded and H_2-loaded fibers, respectively. Solid lines are obtained by a least square fit to the data.

the Ge(1) concentration measured in our fibers exposed to various energy densities. Data are fitted by a linear function with zero intercept, whose slope is found to be $(3.5 \pm 0.5) \times 10^{-18}$ cm^2, the linear correlation coefficient being $r = 0.82$.

The linear relationship allows to infer that the induced absorption is mainly due to Ge(1) center; this finding is consistent with previous literature studies, since the observed spectral profile (Fig. 2) can be interpreted as the tail of the absorption band ascribed to Ge(1), peaked at 4.5 eV with full width at half maximum of 0.9–1.3 eV. The slope represents the absorption cross section σ at 3.1 eV, $\sigma_{3.1} = \Delta\alpha_{3.1}/N$, where N is the total concentration [8, 11, 17, 22, 23, 33]. We acknowledge that the agreement between fit and experimental data may be limited by the presence of other small contributions to induced absorbtion, not taken into account since we have fixed the intercept to zero. This may influence the measured value of σ but does not invalidate the attribution of the observed absorption to Ge(1).

Given that the formation of Ge(1) is the cause of transmission loss under UV irradiation of the singlemode fibers in the investigated spectral range, we examine now the generation mechanism of this defect; this will lead us to discuss, more in general, the generation and transformation processes of the several observed Ge-related species.

As known from ESR studies, Ge(1) is induced by trapping of an electron e$^-$ on a

fourfold coordinated Ge (GeO$_4$) [8, 10]. Hence, the generation of Ge(1) requires ionization of an donor which makes available the electron to be trapped on GeO$_4$ site. A hint on the generation mechanism of Ge(1) comes from Fig. 6(b), where we report the concentration of Ge(1) as a function of Ge(2) as observed in virgin fibers. We see that the growths of the two centers are linearly correlated ($r = 0.98$) with slope $\sim$0.5. This finding, which is peculiar to virgin fibers, suggests that the generation processes of the two defects are actually linked in these materials. The two alternative models proposed for Ge(2) center give rise to two different interpretations for this correlation.

In particular, if we accept the model of Ge(2) as an electron trapping center [10, 26], the correlation can be interpreted as follows: the generation of both defects is driven by trapping of electrons produced by ionization of a common center X (whose structure is unknown at this stage).

$$\mathtt{X + GeO_4 + }h\nu \longrightarrow \mathtt{Ge(2) \ or \ Ge(1)} \tag{1}$$
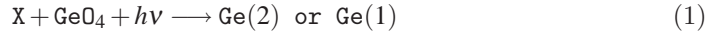
and the slope $\sim$0.5 represents the relative probability of a released electron being trapped on the two precursors giving rise to Ge(1) or Ge(2) (fourfold coordinated Ge with one or two nearest-neighboring Ge atoms respectively).

At variance, assuming the model of Ge(2) as a hole center consisting in an ionized GLPC, $(=\mathrm{Ge}\bullet)^+$ [9, 27, 28], we can suppose that the following mechanism is responsible for the generation of Ge(1):

$$\mathtt{GLPC + GeO_4 + }h\nu \longrightarrow \mathtt{Ge(2) + e^- + GeO_4} \longrightarrow \mathtt{Ge(1) + Ge(2)} \tag{2}$$

i.e. laser-induced ionization of GLPC followed by trapping of the e$^-$ on a fourfold coordinated Ge precursor. In this scheme, the slope $\sim$0.5 represents the probability that an electron released from GLPC encounters a GeO$_4$ site and is trapped on it, while the extra electrons are trapped on unknown centers acting as well as electron traps. We stress that since the GLPC is known to absorb at 5.1 eV and 7.4 eV, its ionization requires at least two Ar$^+$ laser photons. Then, the most probable ionization mechanism is two-step absorption via the intermediate long-lived triplet state, where the center can be excited by resonant 5.1 eV absorption in its B$_{2\beta}$ band followed by intersystem crossing [22]. At variance, the possibility of direct two photon absorption from ground state to conduction band is expected to be very unlikely due to the low intensity of the cw laser radiation.

As regards the loaded fiber, we see that the addition of H$_2$ leads to several effects, which permit to further discuss the issue of the Ge(2) structural model. In fact, the presence of hydrogen causes the disappearance of Ge(2) centers, whereas Ge(1) are detected in comparable concentrations with respect to unloaded fibers (Fig. 3). Hence, our data allow to infer that Ge(2) centers are passivated by reaction with mobile hydrogen. This observation contrasts with the model in which Ge(1) and Ge(2) are both four-fold coordinated Ge electron traps, differing only for the number of nearest-neighboring Ge atoms, because in this case the very similar structures of the two centers should lead to very similar reaction properties with hydrogen. At variance, present results can be easily interpreted on the basis of the *GLPC$^+$* model for Ge(2), whose annealing is due to the following reaction with mobile hydrogen:

$$\mathtt{Ge(2) + H_2 \rightarrow (GLPC{-}H)^+} \tag{3}$$

where the defect at the right side of reaction 3 is an ESR-insensitive diamagnetic center, as already proposed by Fujimaki *et al* [9]. Then, we can suppose that in H$_2$-loaded

samples Ge(1) are still generated by reaction 2, even if Ge(2) are not observed due to reaction 3.

The presence of H_2 gives rise also to the generation of H(II), known to be formed by reaction of hydrogen with GLPC. This can occur either by reaction of GLPC in ground state with H^0 produced by breaking of H_2 on paramagnetic centers [35], or by direct reaction of H_2 with GLPC in excited-triplet state [14, 33]. The latter process leads to an observed reduction of lifetime of GLPC in excited triplet state in presence of H_2 [36]; since we have supposed the generation of Ge(1) to occur by two step absorption of GLPC via the long-lived triplet state, we expect a reduction of the Ge(1) formation rate in presence of hydrogen: this is consistent with the lower initial slope of the H_2-loaded curve in Fig. 3. In this interpretation, it still remains unclear the H_2-induced variation of the saturation value of $\Delta\alpha_{3.1}$.

A further effect of H_2 addition is the strong enhancement of the GeE' creation. This effect has been observed in previous works [37] and may be important for applications as GeE' plays an important role in UV poling of Ge-doped silica leading to induced nonlinearity of the material [2]. Following a model proposed by Awazu *et al.* [37], the increase in the generation efficiency of GeE' in presence of hydrogen may be due to the formation of Ge-H bonds, acting as precursors of the defect. It is interesting to note that the behaviour of GeE' in presence of hydrogen appears very different from that of SiE', the isoelectronic analogous on silicon of the center, which is known to be passivated, and not enhanced, by H_2 diffusion and reaction [38].

5. Conclusions

The UV-induced conversion processes between Ge related point defects were investigated in singlemode optical fibers by the combined use of ESR and OA measurements. The latter were performed by an innovative technique in which the 3.1 eV PL arising from GLPC is used as an intrinsic probe source. The transmission loss of the fibers observed upon UV laser exposure is due to the the tail of a Ge(1)-related absorption band peaked in the UV region. Ge(1) center is generated by trapping on GeO$_4$ sites of electrons produced by ionization of preexisting precursors, GLPC being a possible candidate. In hydrogen-loaded fibers Ge(2) centers are passivated by reaction with H_2. Moreover, the addition of hydrogen enhances the generation efficiency of GeE', leads to formation of H(II) centers, and alters the dependence of induced OA on laser energy density.